Heat Transfer from a Cylinder in an Air-Water Spray Flow Stream

R. LAWRENCE MEDNICK and C. PHILLIP COLVER
The University of Oklahoma, Norman, Oklahoma

Forced convection heat transfer from vertical cylinders normal to an air-water spray flow stream was measured over an air velocity range from 60 to 140 ft./sec. and a water spray density range from 0.03 to 0.50 lb.$_m$/(min.) (sq. in.). Local heat transfer coefficients were determined at 15 deg. intervals around the circumference of both a 1.5 and a 1.0 in. diam. cylinder. It was found that the addition of 0.426 lb.$_m$/(min.) (sq. in.) of water spray to a 133 ft./sec. air stream raised the stagnation point heat transfer coefficient from 45 to 1,650 B.t.u./(hr.) (sq. ft.) (°F.). Similar intensification was found for other angles around the cylinder circumference; however, the magnitude decreased with increasing distance from the stagnation point. Local heat transfer coefficients were normalized with respect to their corresponding stagnation point values and plotted parametrically as a function of angle and air velocity. These profiles showed that the normalized heat transfer coefficients decreased with increasing air velocity at angles other than the stagnation point. Average cylinder heat transfer coefficients were calculated from the air-water data and two correlations were obtained relating these coefficients to the air and the water spray Reynolds number.

In recent years, forced convection heat transfer around submerged bodies has been extensively studied. Although heat transfer from a body submerged in a flowing fluid is a complicated process due to such factors as turbulence, body shape, and flow regime, it is quite well understood for a wide range of these parameters. The addition of a second phase to the flow stream makes the situation extremely complex. In the case of a liquid spray in a gas stream, additional parameters such as droplet size, quality, relative velocities, relative temperatures and relative flow rates could become important. Even with its complexity, such a system merits investigation because of the high heat transfer rates obtainable with relatively small amounts of liquid injected into the gas stream. Information derived from such an investigation can be useful in predicting behaviors in aerodynamic systems as well as in heat exchange equipment.

BACKGROUND

Many investigators (*5, 8, 9, 15, 16, 20*) have studied the Reynolds number effect on heat transfer for a cylinder aligned normal to an air flow stream. Increasing the Reynolds number results in a general increase in the heat transfer rates around the cylinder. The effect of turbulence on heat transfer was studied by several investigators (*8, 12, 21*) for a cylinder in crossflow air. Similar to the Reynolds number effect, increasing free stream turbulence increases the heat transfer rate. Maximum reported heat transfer coefficients for air flow in the subcritical Reynolds number range never exceed 100 B.t.u./(hr.)(sq. ft.) (°F.). Heat transfer to liquid streams from submerged bodies produces considerably higher rates than gases when compared at the same Reynolds number. Fand (*7*), in his study of forced convection around a cylinder, and Brown, Pitts, and Leppert (*2*), in their study of forced convection around a sphere, measured stagnation point heat transfer coefficients of 3,000 B.t.u./(hr.) (sq. ft.) (°F.) at free stream water velocities of 30 ft./sec.

Water spray flowing toward a cylinder in an air-water spray flow stream forms a tangential envelope terminating at the cylinder at an angle less than 90 deg. from the stagnation point. Water spray flowing outside this envelope never impinges the cylinder surface. The tangential angle of intersection with the cylinder is a function of droplet size, droplet velocity, and air velocity. Brun and Mergler (*3*) have theoretically developed local impingement rates over a wide range of the above parameters.

The water spray impinging the cylinder forms a water film, or boundary layer, on the forward portion of the cylinder that flows around the cylinder to the separation point. Here, much of the water leaves the cylinder and flows downstream in the air-water droplet vortices. Also, if the cylinder is in a vertical position, gravity becomes an important force at the separation point and pulls the remaining water down the cylinder wall. The rear portion of the cylinder does not contain a water film, but only occasional droplets splashing back from the vortices. These droplets flow toward the separation point from the rear portion of the cylinder and down the cylinder wall simultaneously. At the separation point, they join with the water film coming from the forward portion of the cylinder and either leave the wall again or flow down the wall.

One of the first heat transfer investigations in spray flow was performed by Tifford (*19*), using a flat plate heater geometry. At about the same time, Acrivos, Ahern, and Nagy (*1*) studied heat transfer from a cylinder to an air-water spray flow stream. Their experimental equipment consisted of a 1.5 in. diam. constant surface temperature cylinder positioned vertically in a horizontal wind tunnel. Results obtained for two air velocities and two spray densities showed as much as an eightfold increase in the local heat transfer coefficients when compared to dry air flow. Later, Hoelscher (*11*) and Takahara (*18*) carried out similar studies using vertically oriented constant temperature cylinders in a horizontal spray flow. Hoelscher specifically studied the effect of increasing water rate on the heat transfer for a single air velocity while the investigation of Takahara covered three air velocities and three water spray densities for each air velocity. Recently, in an air-water spray study, Smith (*17*) has reported stagnation point heat transfer coefficients as high as 1,400 B.t.u./(hr.)(sq. ft.) (°F.) at an air velocity of 63 ft./sec. using a vertical wind tunnel and a horizontal cylinder.

This paper presents the results of an experimental study of heat transfer from constant heat flux cylinders to a horizontal air-water spray flow stream. Previous workers using constant temperature cylinders have experienced difficulty when operating over wide ranges of air velocities and water spray densities. In this study it was the primary purpose to obtain reproducible local heat transfer data over a wide range of air velocities and water spray densities.

R. Lawrence Mednick is presently with Rohm and Haas Company, Philadelphia, Pennsylvania.

EXPERIMENTAL APPARATUS AND PROCEDURE

The apparatus consisted primarily of an electrically heated heat transfer tube, a wind tunnel, a water spray system, a stainless steel demister, and instrumentation. A diagram of the apparatus is shown in Figure 1.

Two thin wall cylinders, electrically heated from a DC power source, were constructed from 1.0 and 1.5 in. diam. stainless steel tubes. Figure 2 is a cross-sectional drawing of the heater assembly. Surface temperatures were measured by three coaxial Chromel-Alumel surface thermocouples, similar to those first used by Moore and Mesler (*14*). Since the surface thermocouple junctions were an integral part of the cylinder surface, the current flowing in the cylinder induced a voltage in the thermocouples. This induced voltage was accurately measured by quickly turning off the heater power and recording the amplitude difference of the surface thermocouple readings on a high-speed recorder. This procedure was first described by Davenport, Magee, and Leppert (*4*). Each heat transfer tube was mounted between copper bus bars which in turn made electrical contact with the DC power leads through amalgamated copper connections. In operation, the heat transfer tube was rotated in 15 deg. increments allowing the surface temperature measurements to be made completely around the circumference. Reference temperature measurements were obtained by the surface thermocouples with the power off. The local heat transfer coefficients were obtained from the corrected local heat flux and the local temperature differences.

The heat transfer tube was located within the test chamber. The test Chamber also housed a traversing mechanism to measure local water spray densities and air velocities over its cross section in a plane perpendicular to the flow stream, 2 in. upstream from the heat transfer tube. Using a method very similar to that used in several previous air-water studies (*1, 11, 17, 18*), water spray densities were measured to a reproducibility of within 3%. The water collection probe essentially consisted of a 0.209 in. I.D. stainless steel, open-ended, L-shaped tube aligned to point directly upstream and connected with flexible tubing to a graduated cylinder. Preliminary tests using an ejector to draw various flow rates through the collection tube gave insignificant variations in results, thus the use of an ejector was discontinued. Air velocities were reproducibly measured to within 2% by using a pitot tube.

The 12 in. diam. wind tunnel contained straightening vanes, honeycomb, and screens to flatten the air velocity profile and eliminate swirling. Water spray, with droplet diameter in the range of 1,200 to 1,800 μ, was injected into the air stream two feet upstream from the heat transfer tube by a Fulljet nozzle. The water spray density was varied by using different size nozzles at 43 lb./sq. in. gauge line pressure. Air velocities were regulated by the use of variable inlet vanes to the blower and a damper duct on the converging section. Entrained liquid water was removed from the exiting flow stream by a stainless steel demister. Screen cylinders located in the demister section were used to break up the high velocity air-water spray flow and evenly distribute the flow to the demister for the removal of the entrained water. A detailed description of the equipment and the experimental procedure is presented elsewhere (*13*).

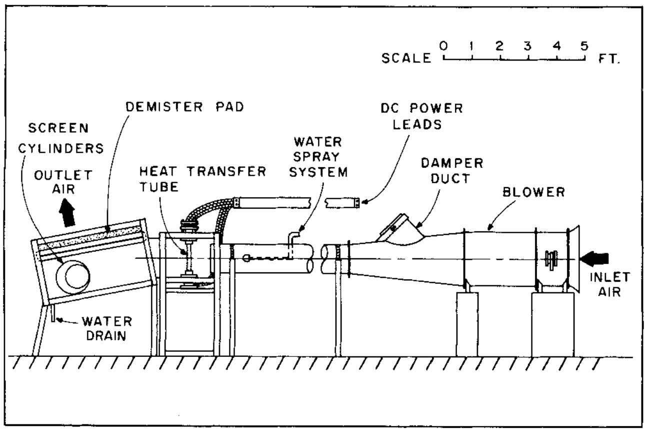

Fig. 1. Diagram of experimental apparatus.

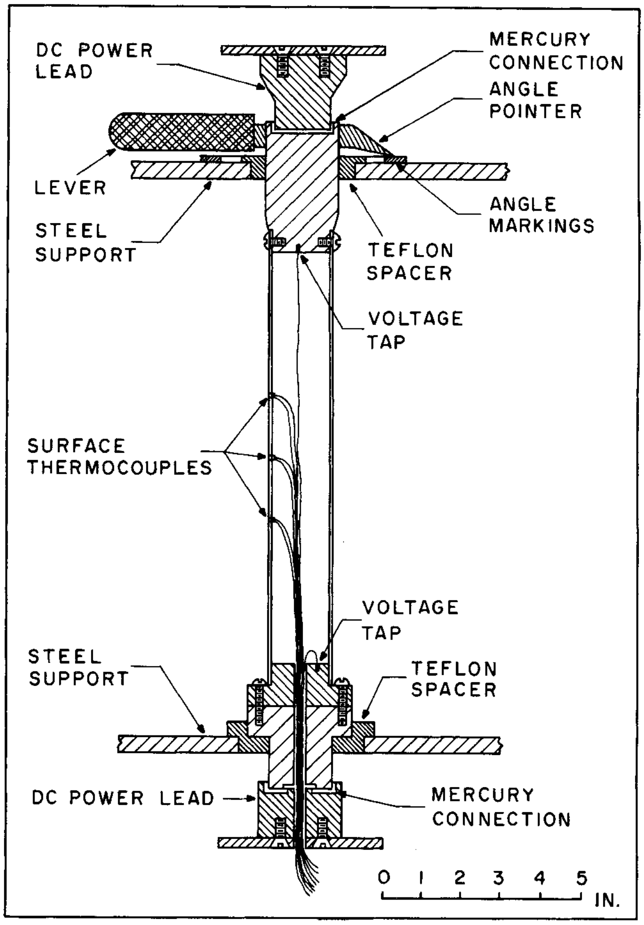

Fig. 2. Heat transfer tube and assembly section view.

EXPERIMENTAL RESULTS

Sixty sets of local heat transfer data were obtained over a range of several spray densities for each of four air velocities from 63 to 133 ft./sec. These data have been tabulated (*13*) for both the 1.5 and the 1.0 in. diam. cylinders. Also included are the water spray and air velocity distributions for each set of data. Air velocities and water spray densities reported in this paper are those measured 2 in. upstream from the forward stagnation point on the heat transfer tube. The air velocity distributions in the plane perpendicular to the flow stream varied no more than 3% from the reported value, while the water spray densities varied no more than 10% from the reported value in the region in front of the heat transfer tube.

Local heat transfer coefficients around the cylinder circumference were calculated from the equation,

$$h = \frac{\dfrac{Q}{A} + kt\ (360/\pi D)^2(\partial^2 T_w/\partial\theta^2)}{T_w - T_o} \tag{1}$$

Here, T_o is the local reference temperature as defined earlier, and was used to obtain heat transfer coefficients which were reproducible and independent of heat flux level at all angles around the cylinder. Since the reference temperature, T_o, was measured locally on the cylinder surface, the temperature difference $T_w - T_o$ was virtually independent of the bulk stream humidity and/or evaporation effects. Further, because of relatively low surface temperatures (<125°F.) encountered over most of the cylinder circumference, any evaporation of water film on the heated cylinder surface was neglected. The second derivative term in Equation (1) is a correction for angular conduction in the tube wall. The maximum value of this correction, which amounted to about 5% of the total

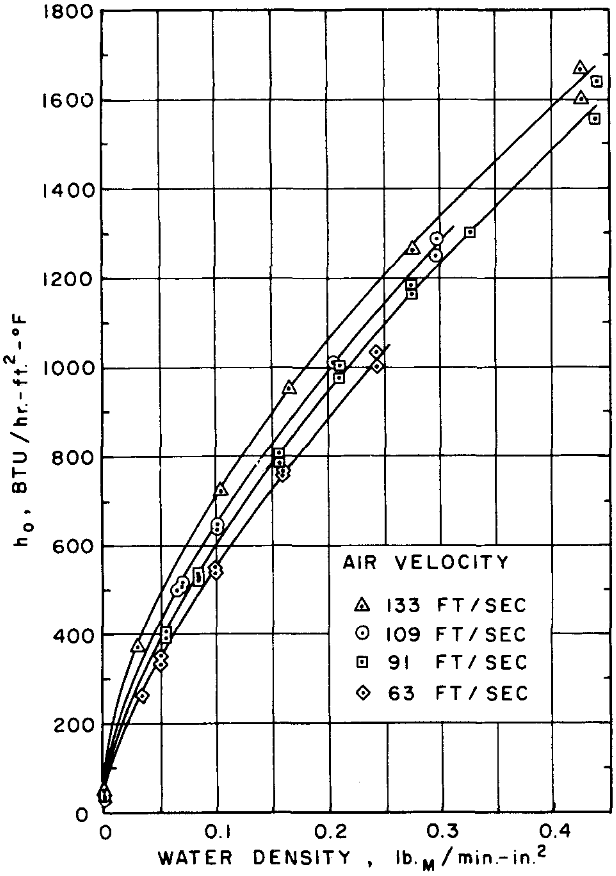

Fig. 3. Stagnation point heat transfer coefficients for 1.5 in. diameter tube.

heat flux, occurred near the separation point and was due to inflections in the temperature profile in this region.

A plot of the stagnation point heat transfer coefficients for the 1.5 in. diam. cylinder is presented in Figure 3. Similar information for the 1.0 in. diam. cylinder is shown in Figure 4. The curves show the heat transfer coefficients plotted with respect to the water spray density, as measured 2 in. upstream from the stagnation point. Data for each of the four experimental air velocities were curve-fitted individually. As seen in the figures, the stagnation point heat transfer coefficient increases with increasing water spray density and increasing air velocity. Each curve originates at its respective value of dry air heat transfer coefficient, increases rapidly through the low water spray density range, and then becomes fairly linear at higher water spray densities. A maximum heat transfer coefficient of 1,760 B.t.u./(hr.) (sq. ft.) (°F.) was measured by using the 1.0 in. diam. cylinder when operating at an air velocity of 133 ft./sec. and a water spray density of 0.38 lb.$_m$/(min.) (sq. in.). At most water spray densities and air velocities, data were taken for two heat fluxes; the resulting stagnation point heat transfer coefficients agreed within 7%.

For any given set of operating conditions, the local surface temperature increased as the cylinder was rotated from the stagnation point. In the region from 90 to 135 deg., the surface temperature reached a maximum. From there, it decreased slightly as the cylinder was rotated toward 180 deg. The reference temperature profile was relatively constant from the forward stagnation point to about 90 deg. and closely matched the water spray droplet temperature measured near the tube. From 90 to 180 deg., the reference temperature dropped as much as 5°F. Finely dispersed water droplets on the rear side of the tube greatly enhanced water evaporation, resulting in the reference temperature approaching the wet-bulb air temperature.

Figure 5 shows a normalized heat transfer coefficient profile for an air velocity of 91 ft./sec. on the 1.5 in. diam. tube. Fourteen individual sets of data for different water spray densities are incorporated in this curve. Local heat transfer coefficients used in determining the normalized plots were values that were averaged from corresponding angles on both sides of the stagnation point. Each of the resulting 0 to 180 deg. profiles was normalized with respect to the stagnation point heat transfer coefficient for that run. For each air velocity, it was found that the normalized profiles were approximately identical over the entire water spray density range studied. All of the normalized profiles determined for a single air velocity are, therefore, fitted with a single curve.

As observed in Figure 5, the normalized heat transfer coefficient rapidly decreases from the stagnation point to about 90 deg. where it is approximately 40% of the stagnation point value. In the region from 0 to 90 deg., a continuous water film existed on the tube surface and, consequently, the heat transfer coefficients were high. Since the thermal boundary layer progressively developed within the water film as the film flowed from the stagnation point to 90 deg., the heat transfer coefficient decreased accordingly. Recall that the heat transfer coefficient is inversely proportional to the thermal boundary layer thickness. From 90 deg. the heat transfer coefficient continued to decrease, but not as rapidly as before. The effect of the separating water film in the region from 90 to 135 deg. caused the intermediate heat transfer coefficients in this range. At 135 deg., the profile essentially leveled out. The region from 135 to 180 deg. was the driest portion of the cylinder and, naturally, yielded the

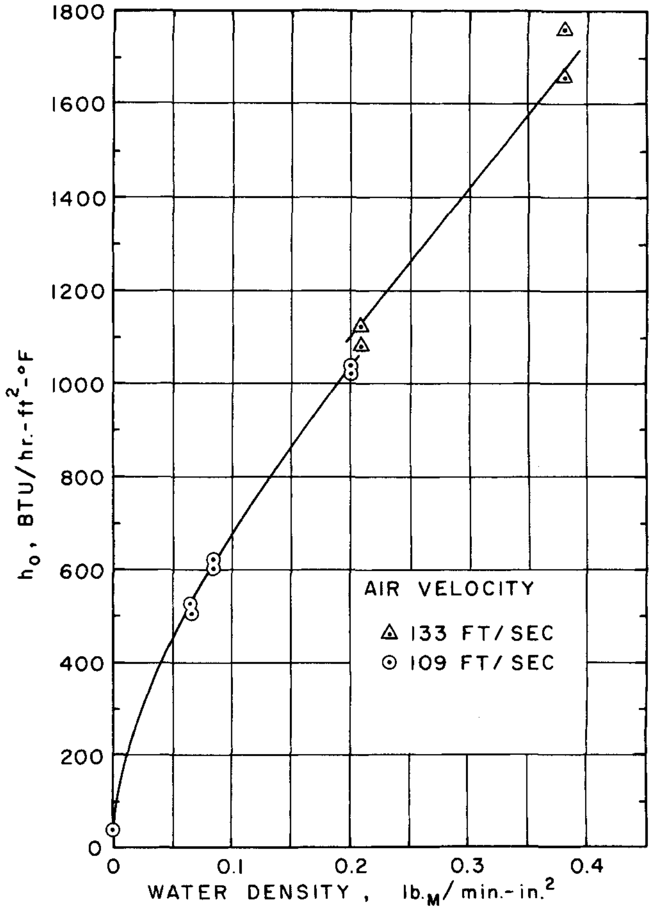

Fig. 4. Stagnation point heat transfer coefficients for 1.0 in. diameter tube.

lowest heat transfer coefficients. Inspection of individual sets of data showed a slight inflection in the heat transfer coefficient profile near 45 deg. Since local temperature and flow measurements were not made within the water boundary layer in this investigation, it was impossible to isolate the exact nature of these observed inflections. However, Brun and Mergler (3) have theoretically shown that in the region from 45 to 75 deg. the flow lines of the water spray become tangent to the cylinder and the liquid film. It is possible that the cessation of water droplet impingement upon the water boundary layer effected a change in the flow characteristics which, in turn, slightly altered the local heat transfer characteristics. Furthermore, since the inflections are similar to those caused by a laminar to turbulent transition in boundary layer flow, it is also possible that such a transition took place in the water film in the region near 45 deg.

Four normalized heat transfer curves which represent all the data taken on the 1.5 in. diam. tube for the four air velocities are shown in Figure 6. Similar information for the 1.0 in. diam. tube is presented in Figure 7. These plots show the effect of increasing air velocity on the heat transfer coefficient profiles. It can be observed that, as the air velocity increases, the normalized profiles decrease more rapidly from the stagnation point. The constant velocity curves are parallel to each other up to about 120 deg., but from 120 to 180 deg., the profiles show no definite pattern due to the erratic behavior of the vortices in this region. The curves show that the inflection at 45 deg. apparently becomes slightly more pronounced with increasing air velocity. Also, the three regions of heat transfer on the cylinder circumference, as described above, show up clearly on all the curves. A comparison of the data for the two tubes shows that increasing the tube diameter has the same effect on the normalized heat transfer coefficient profiles as does increasing air velocity.

CORRELATION OF DATA

Several investigators (*1, 10, 13, 17*) have developed theoretical expressions for the local heat transfer coefficient on the upstream portion of a heated cylinder. In general, the analytical methods have been difficult to apply and, further, require solving numerically with a digital computer. The results can be relied upon to predict actual data only to within an order of magnitude. No reliable analytical methods exist for predicting behavior on the rear portion of a cylinder. Thus, a general correlation of the present experimental data represents the simplest and most fruitful method for obtaining heat transfer information for design purposes.

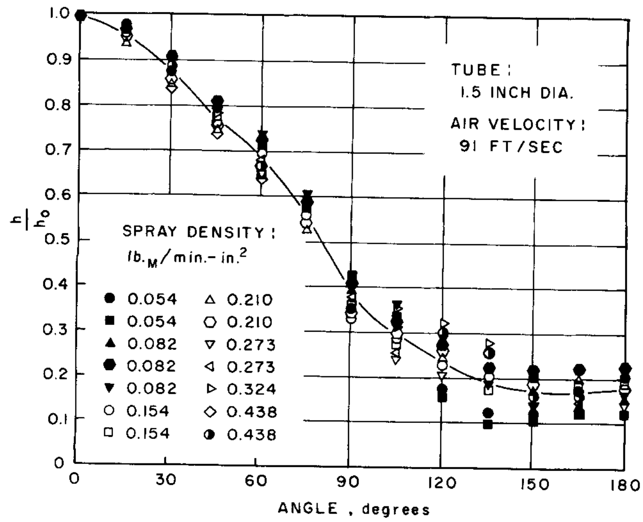

Fig. 5. Normalized heat transfer profile.

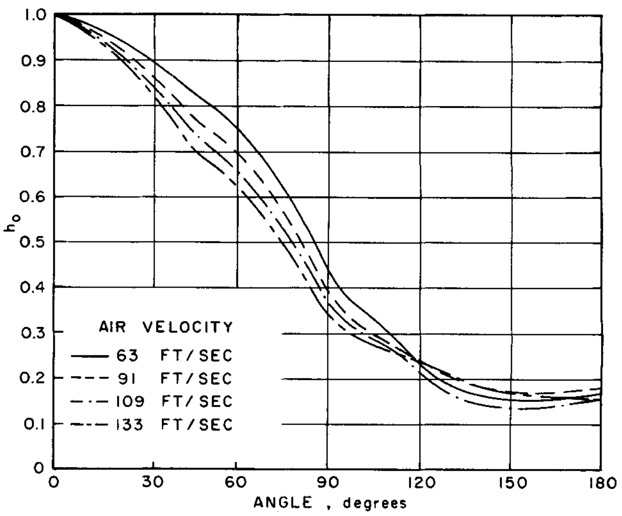

Fig. 6. Normalized profiles for 1.5 in. diameter tube.

The following groups were determined from dimensional analysis.

$$\frac{h_m D}{k_w} = a\left(\frac{WD}{\mu_w}\right)^b \left(\frac{DV\rho_a}{\mu_a}\right)^c \left(\frac{k_w}{c_{pw}\mu_w}\right)^d \left(\frac{\mu_a}{\mu_w}\right)^e \left(\frac{\rho_a}{\rho_w}\right)^f \quad (2)$$

The average cylinder heat transfer coefficient, h_m, was determined by dividing the average cylinder heat flux by the average cylinder temperature difference. Since the data were limited to an air-water flow stream, and since all the data were taken in approximately the same temperature range, it was impossible to isolate the fluid property parameters. Therefore, the last three terms in Equation (2) were incorporated into the constant. The resulting expression can be written as

$$N_{Num} = a\, N_{Re_w}^{\ b}\, N_{Re_a}^{\ c} \quad (3)$$

Correlation of Equation (3) by using average cylinder heat transfer coefficients is shown in Figure 8. The expression which best fits the data is

$$\frac{h_m D}{k_w} = 0.218\left(\frac{WD}{\mu_w}\right)^{0.68} \left(\frac{DV\rho_a}{\mu_a}\right)^{0.27} \quad (4)$$

where the fluid properties were determined at the average surface temperature on the leading half of the cylinder. This particular temperature was used because more than 70% of the heat transfer occurred on the leading half of the cylinder. As can be seen from Figure 8, the range of

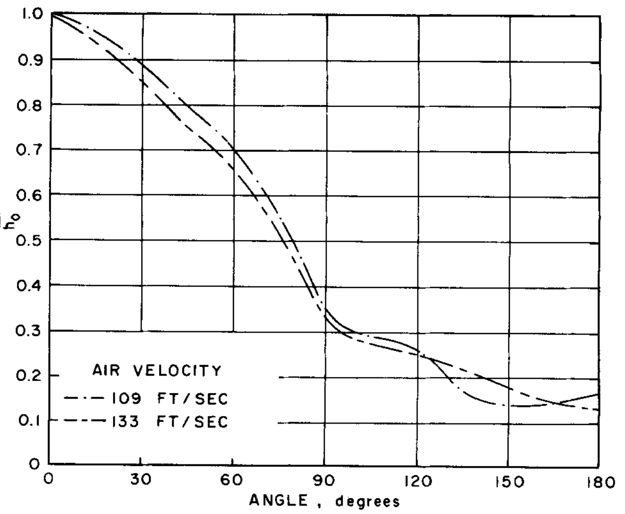

Fig. 7. Normalized profiles for 1.0 in. diameter tube.

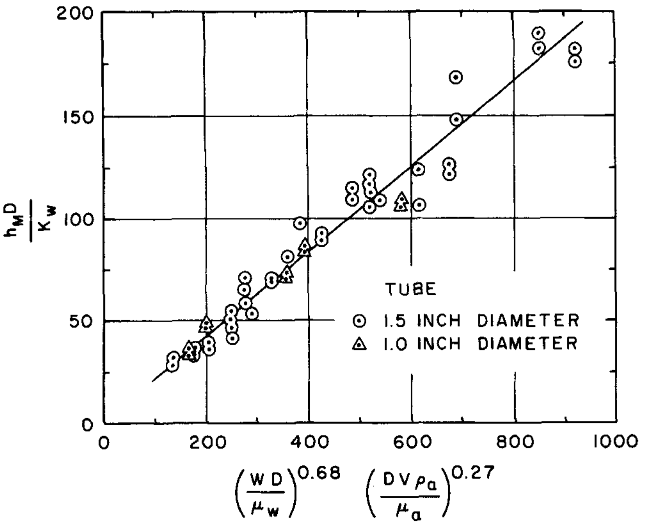

Fig. 8. Correlation of average cylinder heat transfer coefficients.

applicability of the correlation is from 50 to 1,000 on the combined Reynolds numbers raised to their respective powers. Further extension of this range is possible; however, there is no data available for final confirmation.

There is one important limiting case to the above correlation. When the water spray density approaches zero, heat may still be transferred to the dry air flow stream. Equation (4) gives a zero heat transfer coefficient for this limit and, therefore, can not be relied upon for predicting heat transfer coefficients much below the range of experimental spray flow data. However, it was found possible to include terms in the correlation to account for this limit. The air correlation of Douglas and Churchill (6) was chosen to represent the dry air heat transfer in the modified air-water spray flow correlation. The following average heat transfer coefficient correlation was established:

$$\frac{h_m D}{k_w} = \left(\frac{WD}{\mu_w}\right)^{0.65} \left(\frac{DV\rho_a}{\mu_a}\right)^{0.14} + \frac{k_a}{k_w}\left[0.46\left(\frac{DV\rho_a}{\mu_a}\right)^{0.5} + 0.00128\left(\frac{DV\rho_a}{\mu_a}\right)\right] \quad (5)$$

The dry air data and the air-water spray data are compared with Equation (5) in Figure 9.

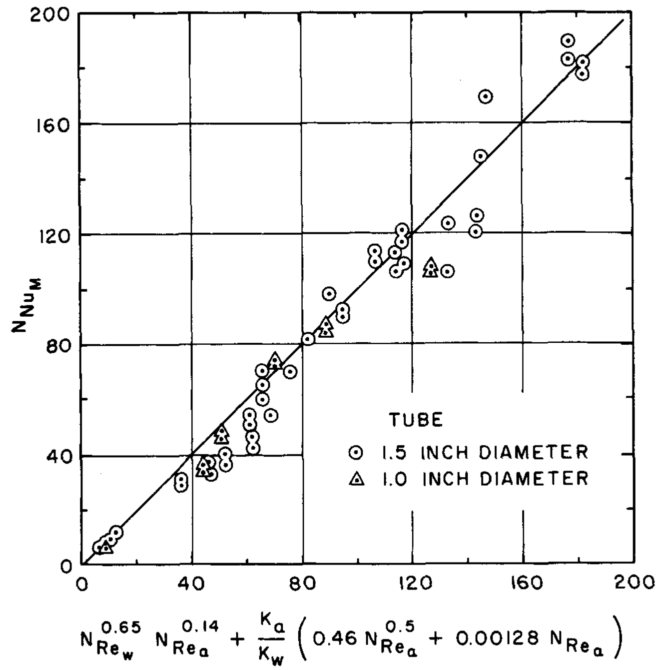

Fig. 9. Correlation of average coefficients including dry air data.

The air-water spray data fit Equation (4) somewhat better than Equation (5); however, Equation (5) correlated the dry air data as well as the air-water spray data. Therefore, each correlation has its advantages. Equation (4) is easier to use and it predicts the average heat transfer coefficients more accurately as long as the water spray density is between 0.03 and 0.50 lb.$_m$/(min.) (sq. in.). Equation (5) has the advantage that it applies over the water spray density range from 0.00 to 0.50 lb.$_m$/(min.) (sq. in.). Both correlations apply over the air velocity range from 63 to 133 ft./sec.

ACKNOWLEDGMENT

R. L. Mednick is indebted to the National Science Foundation for their financial support through a Traineeship. The Otto H. York Company donated the demister for this investigation.

NOTATION

- A = tube surface area, sq. ft.
- c_p = heat capacity, B.t.u./(lb.$_m$) (°F.)
- D = O.D. of cylinder, ft.
- h = local heat transfer coefficient, B.t.u./(hr.) (sq. ft.) (°F.)
- k = thermal conductivity, B.t.u./(hr.) (ft.) (°F.)
- N_{Nu} = Nusselt number, hD/k, dimensionless
- N_{Re} = Reynolds number, $DV\rho/\mu$, dimensionless
- Q = heat flow, B.t.u./hr.
- t = cylinder wall thickness, ft.
- T_o = local reference surface temperature, °F.
- T_w = local tube surface temperature, °F.
- ΔT = $T_w - T_o$, °F.
- V = free stream air velocity, ft./sec.
- W = water spray density, lb.$_m$/(min.) (sq. ft.)
- μ = viscosity
- π = 3.1416
- ρ = density, lb.$_m$/(cu. ft.)
- θ = angle, degrees

Subscripts

- a = air
- m = average over entire cylinder circumference
- o = stagnation point
- w = water

LITERATURE CITED

1. Acrivos, A., J. E. Ahern, and A. R. Nagy, "Research Investigation of Two-Component Heat Transfer," *ARL 64-1161* (1964).
2. Brown, W. S., C. C. Pitts, and G. Leppert, *J. Heat Transfer*, **84**, 133 (1962).
3. Brun, R. J., and H. W. Mergler, *Nat. Advisory Comm. Aeron. TN 2904* (1953).
4. Davenport, M.E., P. M. Magee, and G. Leppert, *J. Heat Transfer*, **84**, 187 (1962).
5. Davies, P. O., and M. J. Fisher, *Proc. Roy. Soc. (London), Ser. A*, **280**, 486 (1964).
6. Douglas, W. J. M., and S. W. Churchill, *Chem. Engr. Progr. Symp. Series*, No. **52**, 23 (1956).
7. Fand, R. M., *Int. J. Heat Mass Transfer*, **8**, 995 (1965).
8. Galloway, T. R., and B. H. Sage, *AIChE J.*, **13**, 563 (1967).
9. Geidt, W. H., *J. Heat Transfer*, **71**, 375 (1949).
10. Goldstein, M. E., Wen-Jei Yang, and J. A. Clark, *ibid.*, **89**, 185 (1967).
11. Hoelscher, J. F., M.S. thesis, Air Force Inst. Tech. (1965).
12. Krestin, J., P. F. Maeder, and H. H. Sogin, *Z. Angew. Math. Phys.*, **12**, 115 (1961).
13. Mednick, R. L., Ph.D. thesis, Univ. Oklahoma, Norman (1967).
14. Moore, F. D., and R. B. Mesler, *AIChE J.*, **7**, 620 (1961).
15. Perkins, H. C., and G. Leppert, *J. Heat Transfer*, **84**, 257

(1962).
16. ———, *Int. J. Heat Mass Transfer*, 7, 143 (1964).
17. Smith, J. W., "Heat Transfer Studies of Water-Spray Flows," *ARL-66-0091* (1966).
18. Takahara, E. W., MS thesis, Air Force Inst. Tech. (1965).
19. Tifford, A. N., "Exploratory Investigation of Laminar Boundary Layer Heat Transfer Coefficients of Gas Liquid-Spray Systems, *ARL 64-136* (1964).
20. Van Meel, D. A., *Int. J. Heat Mass Transfer*, **5**, 715 (1962).
21. Zapp, G. M., MS thesis, Oregon State Univ., (1950).

Manuscript received October 26, 1967; revision received March 13, 1968; paper accepted March 14, 1968. Paper presented at AIChE Los Angeles meeting.

A Thermodynamic Equation Relating Equilibrium Vapor-Liquid Compositions and Enthalpy Differences in Isobaric Multicomponent Systems

LUH C. TAO
University of Nebraska, Lincoln, Nebraska

A rigorous and simple thermodynamic equation relating equilibrium vapor-liquid compositions and the phase enthalpy differences for a binary, isobaric system is extended to multicomponent systems. An analysis is made to indicate the potential applications of computing the latent heat of vaporization directly from the isobaric vapor-liquid equilibrum data and testing the consistency of phase composition and enthalpy data.

Enthalpy information of multicomponent systems is important to the design of distillation equipment, especially for the high pressure, multicomponent systems of which experimental enthalpy studies are costly and combinations of components are numerous. Studies have been made to estimate enthalpy from P-V-T data or equations of state. Papadopoulos, Pigford, and Friend (*1*), and Edmister and Canjar (*3*) used the partial enthalpy calculated from the Benedict-Webb-Rubin equation of state (*2*). Stiehl, Hobson, and Weber (*18*) pointed out the questionable reliability of the B-W-R equation in the liquid phase region; they then suggested the use of differential heat of condensation to estimate the enthalpy of saturated liquid from that of the saturated vapor. Bahlke and Kay (*1*) showed a rigorous method, and Edmister (*4*) proposed an approximate method to calculate the integral heat of condensation.

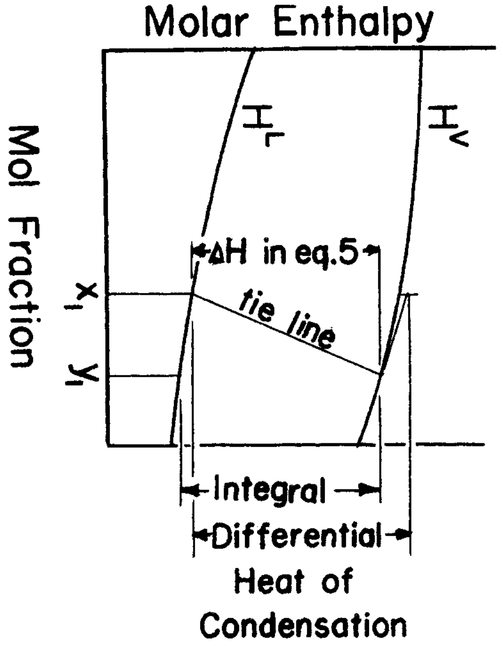

Fig. 1. Various enthalpy differences.

During their search of methods to calculate the vapor composition from the vapor pressure data, Ljunglin and van Ness (*12*, *20*) showed an interesting equation for binary systems to relate the phase enthalpy difference (Figure 1) and x-y-T data. This paper extends their equation to the multicomponent systems, examines the limit forms, and discusses the potential applications of estimating the latent heat directly from x-y-T data, checking the consistency between the phase composition and enthalpy, and estimating the vaporization ratio of a component with several trace components.

THEORY

The unrestricted form of Gibbs-Duhem equation was obtained by Ibl and Dodge for a binary (*9*) and later extended by van Ness (*20*) to a completely unrestricted form for multicomponent systems. For a single phase sys-